Pulse shortening of gain switched single mode semiconductor lasers using a variable delay interferometer

Antonio Consoli* and Ignacio Esquivias

Departamento de Tecnología Fotónica y Bioingeniería - CEMDATIC, Universidad Politécnica de Madrid, Ciudad Universitaria 28040 Madrid, Spain
*antonio.consoli@tfo.upm.es

Abstract: We propose a pulse shaping and shortening technique for pulses generated from gain switched single mode semiconductor lasers, based on a Mach Zehnder interferometer with variable delay. The spectral and temporal characteristics of the pulses obtained with the proposed technique are investigated with numerical simulations. Experiments are performed with a Distributed Feedback laser and a Vertical Cavity Surface Emitting Laser, emitting at 1.5 µm, obtaining pulse duration reduction of 25-30%. The main asset of the proposed technique is that it can be applied to different devices and pulses, taking advantage of the flexibility of the gain switching technique.

©2012 Optical Society of America

OCIS codes: (140.5960) Semiconductor lasers; (140.3490) Lasers, distributed-feedback; (250.7260) Vertical cavity surface emitting lasers; (140.3538) Lasers, pulsed; (320.5540) Pulse shaping; (120.3180) Interferometry.

References and links

1. K. Y. Lau, "Gain switching of semiconductor injection lasers," Appl. Phys. Lett. **52**(4), 257–259 (1988).
2. P. P. Vasil'ev, I. H. White, and J. Gowar, "Fast phenomena in semiconductor lasers," Rep. Prog. Phys. **63**(12), 1997–2042 (2000).
3. P. Paulus, R. Langenhorst, and D. Jager, "Generation and Optimum Control of Picosecond Optical Pulses from Gain-Switched Semiconductor-Lasers," IEEE J. Quantum Electron. **24**(8), 1519–1523 (1988).
4. R. J. Helkey and Y. Arakawa, "Cavity optimization for minimum pulsewidth of gain-switched semiconductor lasers," IEEE Photon. Technol. Lett. **7**(3), 272–274 (1995).
5. A. Takada, T. Sugie, and M. Saruwatari, "High-speed picosecond optical pulse compression from gain-switched 1.3-µm distributed feedback-laser diode (DFB-LD) through highly dispersive single-mode fiber," J. Lightwave Technol. **5**(10), 1525–1533 (1987).
6. H.-F. Liu, Y. Ogawa, and S. Oshiba, "Generation of an extremely short single mode pulse (2 ps) by fiber compression of a gain-switched pulse from a 1.3 µm distributed feedback laser diode," Appl. Phys. Lett. **59**(11), 1284–1286 (1991).
7. D. J. L. Birkin, E. U. Rafailov, W. Sibbett, L. Zhang, Y. Liu, and I. Bennion, "Near-transform-limited picosecond pulses from a gain-switched InGaAs diode laser with fiber Bragg gratings," Appl. Phys. Lett. **79**(2), 151–152 (2001).
8. M. Nakazawa, K. Suzuki, and Y. Kimura, "Transform-limited pulse generation in the gigahertz region from a gain-switched distributed-feedback laser diode using spectral windowing," Opt. Lett. **15**(12), 715–717 (1990).
9. K. Wada, S. Takamatsu, H. Watanebe, T. Matsuyama, and H. Horinaka, "Pulse-shaping of gain-switched pulse from multimode laser diode using fiber Sagnac interferometer," Opt. Express **16**(24), 19872–19881 (2008).
10. C. de Dios and H. Lamela, "Compression and Reshaping of Gain-Switching Low-Quality Pulses Using a Highly Nonlinear Optical Loop Mirror," IEEE Photon. Technol. Lett. **22**(6), 377–379 (2010).
11. K. Wada, Y. Akage, H. Marui, H. Horinaka, N. Yamamoto, and Y. Cho, "Simple method for determining the gain saturation coefficient of a distributed feedback semiconductor laser," Opt. Commun. **130**(1-3), 57–62 (1996).
12. K. Wada and Y. Cho, "Improved expression for the time-bandwidth product of picosecond optical pulses from gain-switched semiconductor lasers," Opt. Lett. **19**(20), 1633–1635 (1994).
13. A. Consoli, J. M. Tijero, and I. Esquivias, "Time resolved chirp measurements of gain switched semiconductor laser using a polarization based optical differentiator," Opt. Express **19**(11), 10805–10812 (2011).

14. J. M. Dudley, L. P. Barry, J. D. Harvey, M. D. Thomson, B. C. Thomsen, P. G. Bollond, and R. Leonhardt, "Complete characterization of ultrashort pulse sources at 1550 nm," IEEE J. Quantum Electron. **35**(4), 441–450 (1999).
15. A. Consoli, I. Esquivias, F. J. L. Hernandez, J. Mulet, and S. Balle, "Characterization of Gain-Switched Pulses From 1.55-μm VCSEL," IEEE Photon. Technol. Lett. **22**(11), 772–774 (2010).

1. Introduction

Short optical pulses with duration of tens of picoseconds can be easily generated from Gain Switched (GS) semiconductor lasers [1] and find application in a rich variety of fields [2]. Pulses from GS lasers are intrinsically characterized with a relevant amount of negative frequency chirp, due to the current induced index modulation around the threshold carrier density value. The limit of the minimum pulse duration that can be obtained is set by the device and the choice of the gain switching parameters [3, 4].

Several techniques for pulse compression and pulse shaping have been developed in order to circumvent this limit and obtain shorter and better shaped pulses. Highly chirped pulses from GS semiconductor lasers can be compressed by the use of a negatively dispersive medium, e.g. an optical fiber [5, 6], or with the design of an optimized Fiber Bragg Grating (FBG), which spectral magnitude and phase profiles are designed to obtain transform limited pulses [7]. Spectral windowing with a Fabry-Perot etalon [8], interferometric spectral filtering [9] and non linear optical loops mirrors [10] have also been successfully employed for pulse shortening of GS lasers.

In general, all the mentioned techniques are *ad hoc* solutions, i. e. given the pulse temporal and spectral characteristics the compression stage works optimally only on the specific pulse it is designed for. As an example, the fiber length or the FBG Transfer Function (TF) must be chosen carefully after a precise time and frequency characterization of the pulse for transform limited compression. This is actually a limitation to the flexibility of the gain switching technique, as a change in the modulation parameters, such as the repetition rate or the modulation amplitude, modifies the spectral and temporal profiles of the pulse. A spectral filter with TF that can be varied according to the pulse characteristics would be a great advantage with respect to the existing pulse shaping techniques from GS lasers.

In this work we present a pulse shortening technique based on a birefringent, Mach Zehnder (MZ) interferometer with variable delay and apply it to the pulses generated from a GS Distributed Feedback (DFB) laser and a Vertical Cavity Surface Emitting Laser (VCSEL), both emitting in the 1.5 μm region. Pulses with different durations are obtained, varying the modulation amplitude in gain switching regime. The interferometer TF is modified accordingly to reduce the pulse duration by varying the difference between the two interferometer arms.

This work is organized as follows: in Section 2, the results obtained after numerical simulation of the proposed technique are presented, in Section 3, the experimental results are described and in Section 4, the main conclusions are drawn, discussing advantages and drawbacks of the technique.

2. Simulation results

In this section, we present the numerical simulations performed in order to test the viability of the proposed technique. We introduce the density rate equations for a single mode semiconductor laser and present the temporal and spectral characteristics of pulses generated in gain switching regime. The pulses obtained are spectrally filtered with a MZ interferometer and simulation results are shown for the case in which the interferometer free spectral range matches the pulse spectrum. The observed reduction of the pulse tail and duration is presented and discussed.

Simulations are performed with the following set of density rate equations:

$$\frac{dN(t)}{dt} = \frac{I(t)}{qV_{act}} - \frac{N(t)}{\tau_N} - v_G \frac{dG}{dN} \frac{(N(t) - N_0)}{1 + \varepsilon S} S(t) \tag{1}$$

$$\frac{dS(t)}{dt} = v_G \Gamma \frac{dG}{dN} \frac{(N(t) - N_0)}{1 + \varepsilon S(t)} S(t) - \frac{S(t)}{\tau_P} + \beta \Gamma \frac{N(t)}{\tau_N} \tag{2}$$

$$\frac{d\varphi(t)}{dt} = \frac{\alpha}{2} \left(v_G \Gamma \frac{dG}{dN} (N(t) - N_0) - \frac{1}{\tau_P} \right) \tag{3}$$

where $N(t)$, $S(t)$ and $\varphi(t)$ are the carrier and photon density and the optical phase, respectively.

The symbol definition of the laser parameters and their values are given in Tab. 1. Values have been optimized in order to have good agreement with the experimental results obtained with the 1550 nm VCSEL.

The current $I(t)$ in Eq. (1) is given by the sum of a direct coupled (DC) term, I_{BIAS}, and a sinusoid with peak to peak amplitude I_{AMP} and oscillation frequency f_{GS}, $I = I_{BIAS} + I_{AMP} \cdot sin(2\pi f_{GS}t)$. I_{BIAS} and I_{AMP} are chosen in order to generate single peaked pulses at a repetition rate of 1 GHz, with similar temporal and spectral characteristics to the pulses obtained in experiments with the VCSEL.

The pulse complex envelope is obtained from $S(t)$ and $\varphi(t)$ taken over one period, as $E(t) = \sqrt{S(t)} \exp(j\phi(t))$, where t is the time variable and j is the imaginary unit. The pulse instantaneous frequency, i. e. the chirp $v(t)$, is obtained from the time derivative of the phase as $v(t) = (2\pi)^{-1} d(\varphi(t))/dt$. The pulse complex spectrum is calculated as $\tilde{E}(f) = FT[E(t)]$, where FT is the Fourier Transform operator and f the frequency domain variable.

Table 1. 1550 nm VCSEL Parameters

Symbol	Definition	Value	Units
q	Electron charge	$1.602 \cdot 10^{-19}$	C
V_{act}	Active volume	$3.12 \cdot 10^{-12}$	cm^3
Γ	Confinement factor	0.02	-
dG/dN	Differential gain	$1.6 \cdot 10^{-16}$	cm^2
v_G	Group velocity	$9.4 \cdot 10^9$	cm/s
N_0	Transparency carrier density	$1.61 \cdot 10^{18}$	cm^{-3}
τ_N	Carrier lifetime	1	ns
τ_P	Photon lifetime	5.5	ps
ε	Nonlinear gain compression factor	$1 \cdot 10^{-17}$	cm^3
β	Spontaneous emission coefficient	$1e^{-5}$	-
α	Linewidth enhancement factor	5.9	-
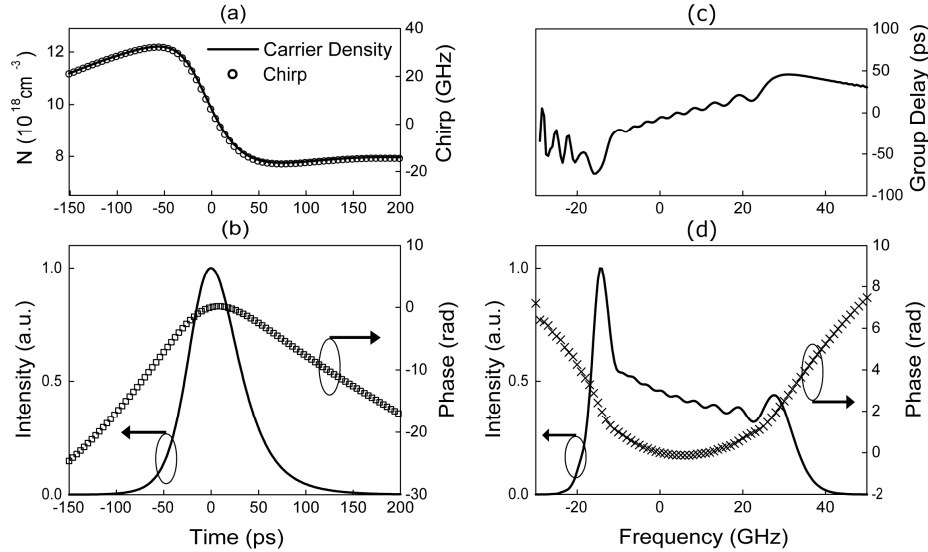
Fig. 1. Simulations results obtained with f_{GS} = 1 GHz, I_{BIAS} = 1.5 I_{TH} and I_{AMP} = 4 I_{TH}: carrier density and chirp temporal profiles, (a), pulse intensity and phase versus time, (b), group delay, (c) and pulse spectral intensity and phase, (d).

Simulations have been performed with f_{GS} = 1 GHz, I_{BIAS} = 1.5 I_{TH} and I_{AMP} = 4 I_{TH}, where I_{TH} is the laser threshold current (2 mA in the VCSEL under study). Figure 1 shows the simulation results in time, Figs. 1(a) and 1(b), and frequency, Figs. 1(c) and 1(d). The expected carrier induced frequency chirp is clearly shown in Fig. 1(a), where the carrier density and chirp temporal profiles are plotted. Instantaneous frequency decreases rapidly and almost linearly in coincidence of the pulse peak, leading to quasi quadratic temporal and spectral phase profiles, shown in Figs. 1(b) and 1(d), respectively. The spectral intensity is asymmetric with a peak on the lower frequencies side and a broadened weaker spectrum on the higher frequency side, see Fig. 1(d). The spectrum is characterized with a quasi-periodic structure which has been reported in previous works on GS lasers both theoretically [11, 12] and experimentally [5]. This is understood as the spectral signature of the relaxation oscillations at these gain switching conditions. In Fig. 1(c) the group delay, t_d, calculated as the time derivative of the spectral phase, is plotted.

As shown in Fig. 1(d), the spectrum has an asymmetric intensity profile characterized by a peak on the lower frequencies side and a broadened "shoulder" profile on the higher frequencies side. These correspond to the falling and rising edges of the pulse, respectively, as predicted by theory [11, 12] and confirmed with experiments [13, 14]. According to this, spectral filtering can be used for shaping the pulse edges in the temporal domain.

The interferometer TF is calculated in order to contain the pulse spectrum between two adjacent zeros: a maximum of transmission centers the blue side "shoulder" of the pulse spectrum and a minimum is placed close to the red frequencies peak. In this way, the pulse tail is shortened, the rising edge results stepper and the total Full Width Half Maximum (FWHM) duration is reduced. The spectral TF, $H(f)$, of a 50:50 MZ interferometer is numerically implemented with $H(f) = 0.5(1 + exp(j2\pi f\tau))$, where τ is the temporal delay difference between the two interferometer arms. In simulations, the pulse spectrum at the output of the interferometer is calculated as $\tilde{E}_{OUT}(f) = \tilde{E}(f)H(f)$ and its temporal complex envelope, $E_{OUT}(t)$, is obtained after Inverse Fourier Transforming (IFT), as $E_{OUT}(t) = IFT[\tilde{E}_{OUT}(f)]$.
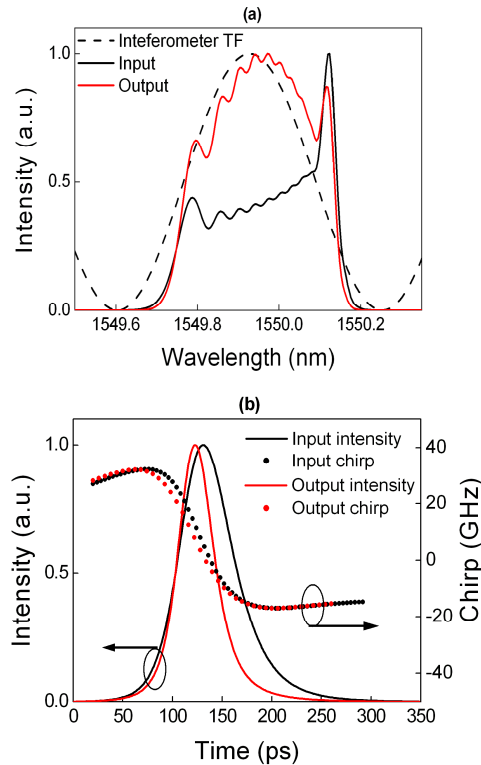
Fig. 2. Simulation results with $f_{GS} = 1$ GHz, $I_{BIAS} = 1.5$ I_{TH} and $I_{AMP} = 4$ I_{TH} and $\tau = 12.317$ ps. (a): normalized pulse spectra at the input (black line) and at the output (red line) of the interferometer and interferometer TF (dashed line). (b): normalized intensity and chirp temporal profiles of the pulse at the input (black line and dots) and at the output (red line and dots) of the interferometer.

Figures 2(a) and 2(b) show the simulation results obtained with $\tau = 12.317$ ps, which corresponds to two zeros of transmission at 1549.6 nm and 1550.25 nm, for the same pulse shown in Fig. 1. The pulse spectral profile at the output of the interferometer is symmetrical with respect to its center, with a FWHM bandwidth of 0.36 nm and a $1/e^2$ bandwidth of 0.42 nm. The spectral power has been calculated as the integral of the spectrum over the entire frequency range before and after the interferometer, resulting in a spectral energy reduction of about 66%. The temporal intensity profile is modified accordingly to spectral filtering, as shown in Fig. 2(b), resulting in a decrease of the pulse FWHM duration from 62 ps to 41 ps. This is due to the attenuation of lower frequencies peak in the spectrum, which corresponds to a reduction of the pulse tail and the total pulse duration. In Fig. 2(b), the chirp profile of the pulse before and after the interferometer is also shown. The total amount of chirp is almost the same before and after the interferometer and the temporal distribution of instantaneous frequency is changed accordingly to spectral filtering.

With the aim of investigating the effect of the delay τ on the output pulse shape, simulations have been performed with different values of τ, showing that shorter pulses can be obtained at expenses of transmitted power. As an example, if the two adjacent zeros of the interferometer TF are placed inside the pulse spectrum, thus performing spectral windowing of the pulse, the output pulse duration is shortened, the peak intensity is reduced and satellite pulses appear before and after the main peak. A detailed study of the pulse shape that can be obtained with different delays is out of the intention of this work. Here we focused our

attention on the flexibility of the proposed method to be applied to different pulses and devices as described in detail in the next section.

3. Experimental results

The proposed pulse shaping technique is applied to a VCSEL and a DFB laser, both emitting in the 1.5 μm region. The set-up is shown in Fig. 3.

Pulses generated from the GS laser diode (GS LD) enter a 50:50 2x2 coupler and travel two different paths: one is directly connected to a 20 GHz photodiode (PD) and channel 1 (CH1) of the oscilloscope (Tektronix DSA8200) and the other enters the interferometer before being detected with a 45 GHz photodiode (New Focus 1014) at channel 2 (CH 2) of the oscilloscope (OSC). In this way, the original and the filtered pulse temporal profiles can be measured at the same time. An Optical Spectrum Analyzer (OSA, Ando AQ6315B) with 6.25 GHz resolution, not shown in figure, has been also used.

On the interferometer path, light from the GS laser is amplified and its polarization state is modified in order to enter the birefringent interferometer with the required linear polarization orientation. Light passes through a Polarization Controller (PC), an Erbium Doped Fiber Amplifier (EDFA), a linear polarizer (P1) and a half wave plate (HWP) before entering the interferometer.

The PC is adjusted accordingly to the laser in use, as the DFB and the VCSEL have different polarization states. In particular, the VCSEL has two orthogonal polarization modes, and the suppressed polarization is enhanced by gain switching operation [15]. Thus, the linear polarizer P1 is used to select only the dominant polarization of the VCSEL.

The EDFA plays a double role in our experiments: it improves the signal to noise ratio and allows the measurement of the interferometer TF over a 40 nm wavelength range, by using its Amplified Spontaneous Emission (ASE) as input signal.
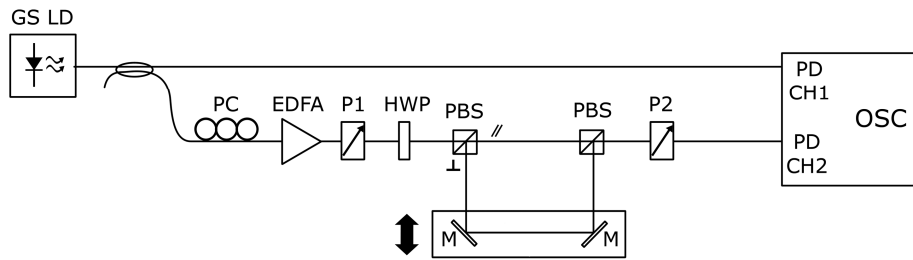
Fig. 3. Experimental set-up. Detailed description is given in the text.

The birefringent interferometer is composed of a first Polarization Beam Splitter (PBS), a motorized translation stage, a second PBS and a linear polarizer (P2). The two PBSs and the translation stage are mounted and sealed in a commercially available device (Differential Polarization Delay Line, OZ Optics). Linearly polarized light enters into the first PBS with a polarization direction oriented at 45° with respect to the PBS axes, which is adjusted by rotating the HWP. The parallel and orthogonal components exit the PBS and travel two different optical paths (the two interferometer arms) before entering the second PBS. One of the two arms is composed of two mirrors (M) mounted on a translation stage which can be moved by a computer controlled step motor. This allows varying the delay between the two arms with a resolution of 3 fs. The parallel and orthogonal components exit the second PBS and interfere at the linear polarizer (P2) oriented at 45° with respect to the PBS axes.

In order to demonstrate that the proposed technique can be applied to different devices and pulses, the same set-up is used to shorten the pulses generated from a GS VCSEL and a GS DFB laser emitting around 1550 nm and 1540 nm, respectively. The heat sink temperature

of the lasers is controlled with a Thermo Electric Cooler (TEC) at a constant temperature of 25°C for all the experiments.

The VCSEL (Raycan) is GS with a DC current I_{BIAS} = 1.6 I_{TH} and a Radio Frequency (RF) sinusoidal current with amplitude, P_{RF}, of 14 dBm at 1 GHz repetition rate and pulses with FWHM duration of 62 ps are obtained. The central wavelength of the spectrum is 1550.9 nm and the spectral bandwidth measured at $1/e^2$ of the maximum is 0.44 nm, showing good agreement with the simulation results presented in Fig. 1. The quasi periodic structure of the spectrum in Fig. 1(d) is lost in measurements, due to the limited resolution bandwidth of the OSA (6.25 GHz). The delay τ is set to τ = 13.14 ps in order to place two adjacent minima in the interferometer TF at 1550.48 nm and 1551.09 nm. The measured interferometer TF, the input and output intensity spectra of the pulses are shown in Fig. 4(a).
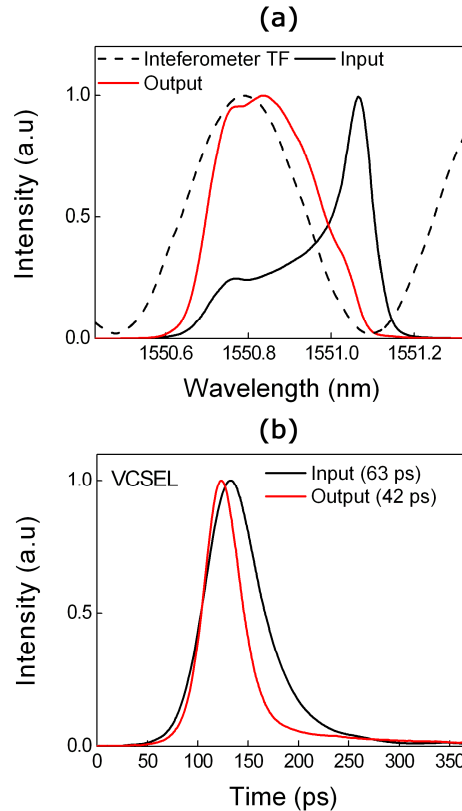
Fig. 4. Experimental results obtained with the VCSEL, for I_{BIAS} = 1.6 I_{TH}, P_{RF} = 14 dBm at 1 GHz. (a): pulse spectra at the input (black line) and output (red line) of the interferometer and interferometer TF (dashed line). (b): pulse temporal profile at the input (black line) and output (red line) of the interferometer.

The original and filtered pulse intensity temporal profiles are shown in Fig. 4(b), the pulse FWHM duration of 63 ps is reduced to 42 ps, thus reaching a 33.3% shorter pulse at the interferometer output. To the best of our knowledge, these are the shortest pulse obtained in GS 1550 nm VCSEL. The intensity loss due to the spectral filtering of the interferometer are obtained by measuring the pulse peak amplitude after polarizer P1 (input pulse) and after P2 (output pulse) and by removing the EDFA from the set-up (see Fig. 3). The original pulse peak amplitude of 1.3 mW is reduced to 0.52 mW at the interferometer output.

The DFB laser (JDS Uniphase) is GS with I_{BIAS} = 1.1 I_{TH} and P_{RF} = 17 dBm at 1 GHz repetition rate, producing pulses with duration of 40 ps. The delay is set to τ = 13.163 ps in

order to have two adjacent minima in the interferometer TF at 1539.25 nm and 1539.85 nm. Figure 5(a) shows the measured spectral profiles and the interferometer TF and Fig. 5(b) shows the input and output pulse spectra. The original pulse FWHM duration of 40 ps is shortened to 29 ps, thus reducing the pulse duration of 27.5%. The original pulse peak intensity of 3.5 mW is reduced to 1.4 mW at the interferometer output. Due to the shorter pulse duration obtained from the GS DFB laser in comparison with the VCSEL, the 45 GHz bandwidth photodetector has been used in the experiments performed with the DFB laser, for measuring both the pulses at the input and output of the interferometer.
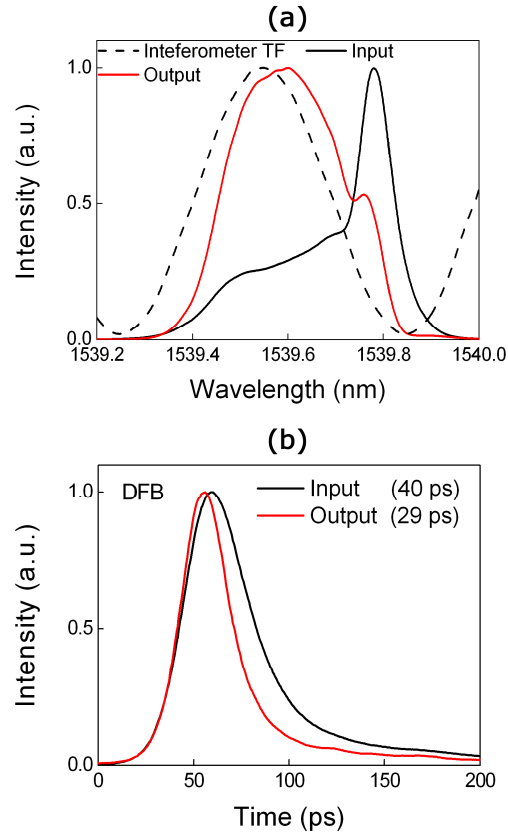
Fig. 5. Experimental results obtained with the DFB laser, for $I_{BIAS} = 1.1$ I_{TH}, $P_{RF} = 17$ dBm at 1 GHz. (a): pulse spectra at the input (black line) and output (red line) of the interferometer and interferometer TF (dashed line). (b): pulse temporal profile at the input (black line) and output (red line) of the interferometer.

In order to demonstrate that the proposed technique can be applied to pulses with different temporal and spectral characteristics, experiments were performed with different gain switching parameters. The bias current and repetition frequency were kept fixed and the modulation amplitude P_{RF} was increased, reducing the pulse duration and increasing the chirp variation.

In the experiments performed with the DFB laser, $I_{BIAS} = 1.1$ I_{TH} ($I_{TH} = 13$ mA), $f_{GS} = 1$ GHz and P_{RF} is varied between 7 dBm and 17 dBm. The results are shown in Fig. 6(a). In Fig. 6(b), the pulse durations obtained with the GS VCSEL with $I_{BIAS} = 1.6$ I_{TH}, $f_{GS} = 1$ GHz and varying P_{RF} between 3 dBm and 14 dBm are shown. An increase of P_{RF} results in a wider spectral bandwidth, due to the increased instantaneous frequency excursion, and in a red shift of the central wavelength of the spectrum, because of the current induced thermal heating of

the device. The delay τ is calculated as previously described in Section 2, for each value of P_{RF}, and the original pulse duration is reduced in the DFB laser and the VCSEL, see Figs. 6(a) and 6(b), respectively. As expected, the shortest pulses are obtained at the highest value of P_{RF}. Their temporal and spectral profiles are shown in Fig. 4 and Fig. 5, for the VCSEL and the DFB laser, respectively.

Shorter durations can be obtained by spectral windowing of the pulse spectrum: if two adjacent zeros are placed close inside the pulse spectrum, shorter pulses are obtained, at expenses of the pulse shape, as satellite pulses appear before and after the main peak.
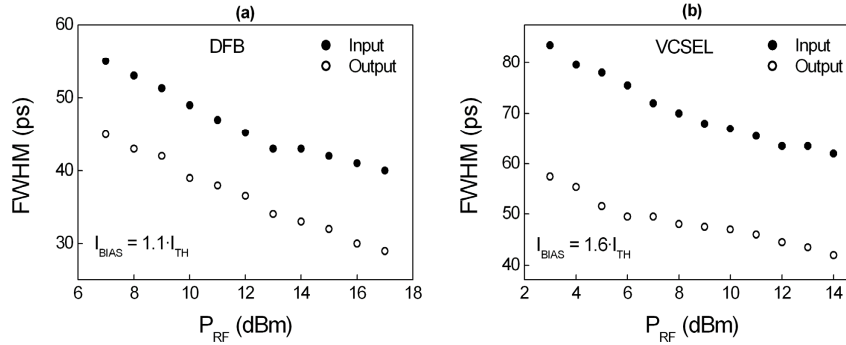
Fig. 6. Pulse durations obtained with the GS DFB laser (a) and the GS VCSEL (b) as a function of P_{RF}, measured at the input (solid dots) and output (hollow circles) of the interferometer. For both lasers, $f_{GS} = 1$ GHz and $I_{BIAS} = 1.1$ I_{TH} and $I_{BIAS} = 1.6$ I_{TH}, for the DFB laser and the VCSEL, respectively.

4. Conclusions

We have confirmed, with simulations and experiments, that a Mach Zehnder interferometer with variable delay can be used for reducing the duration of pulses obtained with GS single mode semiconductor lasers. The variable delay is opportunely set in order to reshape the pulse spectrum, shortening the pulse FWHM duration and tail. An advantage of the proposed technique is that it can be applied to different devices and pulses, by simply varying the delay between the two interferometer arms.

Experiments have been performed with a GS VCSEL and a GS DFB laser, both emitting in the 1.5μm region. The modulation amplitude in gain switching regime has been changed, resulting in pulses with different temporal duration, spectral bandwidth and central wavelength. For all the generated pulses, a reduction of about the 25-30% of the original duration has been obtained, from the DFB laser and the VCSEL, by properly setting the variable delay of the interferometer. An intrinsic limitation of the proposed technique is the intensity loss due to amplitude spectral filtering, in contrast to only phase filtering compression methods, such as pulse compression based on FBG or fiber dispersion. In the performed experiments the pulse attenuation at the output of the interferometer has been measured, giving a relatively small factor of about 0.4.